15th Int Symp on Applications of Laser Techniques to Fluid Mechanics
Lisbon, Portugal, 05-08 July, 2010
Paper 1546

Boundary Layer Measurements in a Supersonic Wind Tunnel Using Doppler Global Velocimetry

James F. Meyers[1], Joseph W. Lee[2], Angelo A. Cavone[3]

1: Distinguished Research Associate of NASA Langley Research Center, Hampton, Virginia 23681, United States james.f.meyers@nasa.gov
(currently: Analytical Services & Materials, Inc., Hampton, Virginia)
2: NASA Langley Research Center, Hampton, Virginia 23681, United States
joseph.w.lee@nasa.gov
3: Alliant Techsystem, Inc., NASA Langley Research Center, Hampton, Virginia 23681, United States angelo.a.cavone@nasa.gov

Abstract A modified Doppler Global Velocimeter (DGV) was developed to measure the velocity within the boundary layer above a flat plate in a supersonic flow. Classic laser velocimetry (LV) approaches could not be used since the model surface was composed of a glass-ceramic insulator in support of heat-transfer measurements. Since surface flare limited the use of external LV techniques and windows placed in the model would change the heat transfer characteristics of the flat plate, a novel approach was developed. The input laser beam was divided into nine equal power beams and each transmitted through optical fibers to a small cavity within the model. The beams were then directed through 1.6-mm diameter orifices to form a series of orthogonal beams emitted from the model and aligned with the tunnel centerline to approximate a laser light sheet. Scattered light from 0.1-micron diameter water condensation ice crystals was collected by four 5-mm diameter lenses and transmitted by their respective optical fiber bundles to terminate at the image plane of a standard two-camera DGV receiver. Flow measurements were made over a range from 0.5-mm above the surface to the freestream at Mach 3.51 in steady state and heat pulse injected flows. This technique provides a unique option for measuring boundary layers in supersonic flows where seeding the flow is problematic or where the experimental apparatus does not provide the optical access required by other techniques.

1. Introduction

To determine the influence of the flow field on heat transfer at supersonic speeds, an investigation was conducted to measure the velocity within a boundary layer above a flat plate at Mach numbers up to 3.51. The challenge was to obtain these velocity measurements as close to the surface as possible within the constraints imposed by the tunnel configuration and the model. The model, shown in Figure 1, was a sharp leading edge flat plate with a 150-mm long, 6-degree bevel. The center of the leading edge was a 361-mm wide section orthogonal to the flow incorporating a 60-degree downstream sweep on each side reaching a total width of 873-mm. The model was oriented at zero degrees angle of attack with no side slip. A 364-mm long by 182-mm wide glass-ceramic insulator (MACOR) insert was placed 242 mm downstream from the leading edge of the flat plate. When the desired run conditions were established, a heat pulse was injected into the flow to provide sufficient

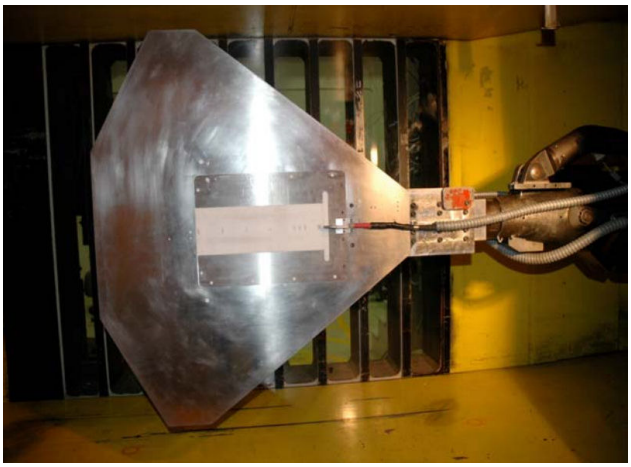

Figure 1.- Flat plate model with MACOR insert.

surface temperature rise over 40 seconds to allow determination of the surface heat transfer. The objective of the flow-field measurements was to document the velocity field from the surface to free stream as a function of time during the passage of the heat pulse.

The investigation was conducted in the Langley Unitary Plan Wind Tunnel (UPWT). UPWT is a closed-circuit, continuous-flow, variable-density supersonic wind tunnel with two test sections: one with a design Mach number range from 1.5 to 2.9 and the other from Mach 2.3 to 4.6. The two test sections are nominally 1.2-x 1.2-m in cross section and 2.1-m in length. Each test section has removable doors on both sides of the test section. The doors can be solid for mounting traversing mechanisms or instrumentation. A single (nominally) 30-mm diameter port can be located in various positions in the solid door for viewing purposes. In addition, a door consisting of nine 230- x 1200-mm rectangular windows separated by 25-mm thick by 230-mm wide reinforcement ribs is available for techniques requiring greater optical access (Figure 1). The investigation was conducted in two parts: Mach 1.51 and 2.16 in the low-speed test section and Mach 3.51 in the high-speed test section.

The choice of flow measurement technology was limited to laser velocimetry techniques so as to not interfere with the flow field and potentially affect the heat transfer from the flow to the surface. Several optical measurement techniques previously used for boundary layer investigations were considered, especially the newly developed diverging/converging fringe laser velocimeter by Lowe and Simpson (2009). This technique provides three-component velocity measurements with micron spatial resolution and yields the ability to measure acceleration and particle trajectory along with velocity. However, the technique has not been used in supersonic flows. It also requires micron-sized particles that will exhibit unknown measurement errors resulting from particle lag, a large cavity within the model to hold the optics, and a relatively large viewing window in the model surface. Since the flat plate model has a small cavity and the installation of a window within the MACOR insulator would affect the heat transfer characteristics of the model, other techniques were investigated.

A review of other laser velocimetry techniques for use in boundary layer investigations suggested that experiments conducted by Mangalam *et al* (1985) using a modified Laser Doppler Velocimeter (LDV) and Brummund and Scheel (2000) using a Laser Two-Focus (L2F) system were possible candidates for obtaining the desired velocity profiles. While the results of these investigations were impressive, the techniques still required the injection of micron-sized particles and potentially introduced significant surface flare that could compromise measurement accuracy. The need to inject particles into the flow can be eliminated using Laser-Induced Thermal Acoustics (LITA), Herring (2008); however, the requirement for optical access on both sides of the test section could not be satisfied given the test constraints. Additionally, these techniques are point measurement systems that cannot simultaneously measure the flow field from the surface to free stream to yield the required time resolved flow characteristics as the heat pulse traverses through the test section.

Planar laser velocimetry techniques such as Particle Image Velocimetry (PIV) (Raffel *et al* (1998, 2007)), Doppler Picture Velocimetry (DPV) (Seiler *et al* (2003)), and Doppler Global Velocimetry (DGV) (Meyers *et al* (2007)) were also examined for this investigation. Unfortunately all three techniques used in their traditional configurations would introduce significant surface flare where the light sheet impacts the model, resulting in compromised measurement accuracy. This problem can be eliminated with the transmission of the light sheet from within the model. But, as stated above, the insertion of a large window in the MACOR panel would compromise the heat-transfer measurements. Further, the transmission of high-energy pulsed laser light through an optical fiber is not possible with today's technology. However, an alternate implementation of DGV using a

continuous-wave laser and optical fibers capable of transmitting sufficient laser energy to make these measurements was possible. A scheme employing a series of equally spaced laser beams projected out from inside the model orthogonal to the surface through orifices equivalent in size (1.6 mm) to surface pressure ports results in an approximation of a light sheet. This arrangement would only provide a discrete sampling of the flow in the streamwise direction, but would yield a continuous three-component measure of velocity through the boundary layer to freestream at the sampling points. Given the test constraints, this approach appeared to have the best chance of success, and was thus chosen.

2. Description of the Optical System

With DGV technology being selected as the approach having the best chance of making the boundary layer measurements, a system was designed for production testing based on the approach used by Meyers *et al* (2005, 2006). The transmission system consisted of a beam-splitting optical system, Figure 2, which transmitted laser beams of equal power down nine optical fibers that were routed to the cavity within the model. Collimators and miniature prisms were used to reform the laser beams and direct them through respective 1.6-mm diameter orifices to yield a fence of laser beams emanating orthogonal from the model surface, Figure 3.

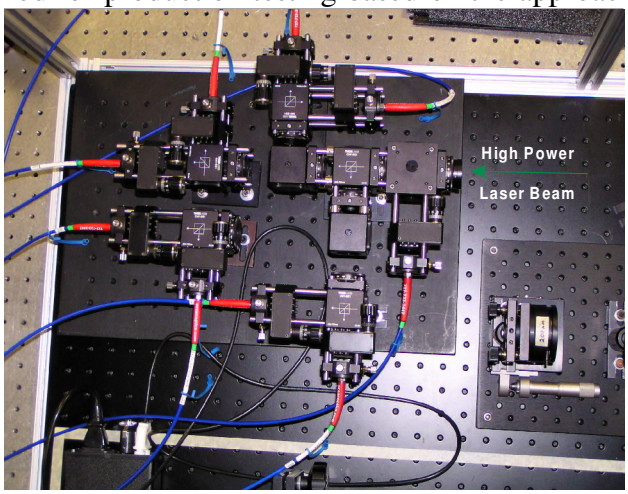

Figure 2.- Beamsplitter and fiber-optic launchers.

As with the previous investigations by Meyers *et al* (2005, 2006), scattered light from particles passing through the laser beams was collected by fiber optic imaging bundles with 5-mm diameter collecting lenses and transmitted to a single, two-camera receiver system. An over-specified, four-component system consisting of four optical fiber bundles and a multi-mode single core fiber for the transmission of a portion of the input laser beam for use as an optical frequency reference was constructed, Figure 4. The proximal ends of the four fiber bundles and the single core fiber were gathered and placed in the imaging plane of the receiver system, Figure 5. This approach provided a direct view of a 350-x 350-mm common area anywhere within the test section. The use of four viewing angles increased measurement accuracy with no compromise on viewing area or spatial resolution. A single vapor-limited Iodine cell was used to

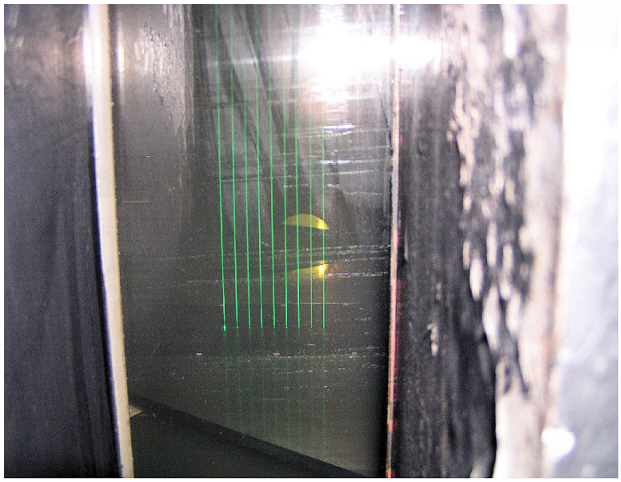
Figure 3.- Laser beam fence.

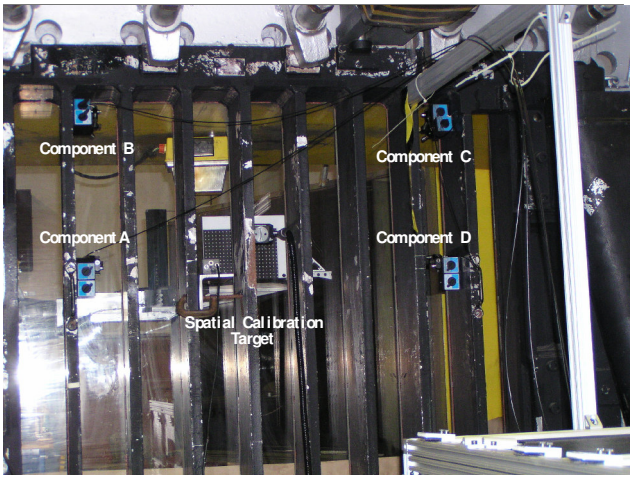

Figure 4.- Optical fiber receiver configuration.

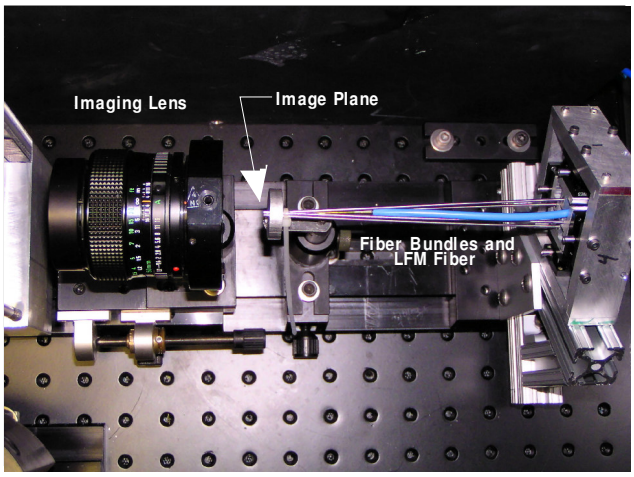

Figure 5.- Image transfer from fiber bundles to DGV.

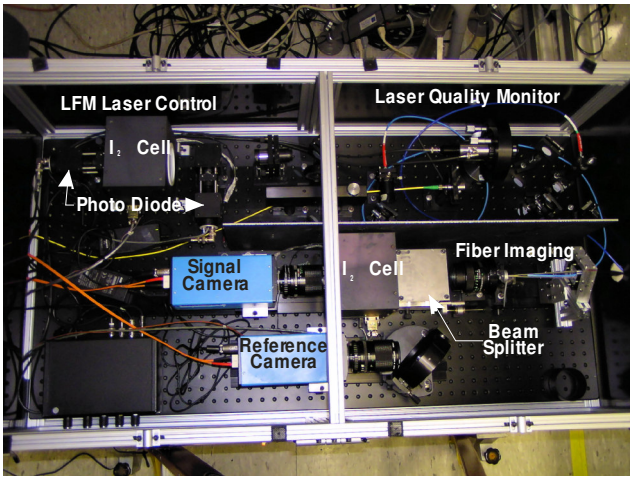

Figure 6.- DGV receiver system and laser frequency monitor.

measure all four velocity components along with the input laser frequency, Figure 6. However, due to the large f-number of the collecting lenses on the distal ends of each fiber bundle, Figure 7, integration times of 1-second were required to obtain sufficient photons for accurate measurements from the sub 0.1-micron water condensation (ice) particles used as the scattering medium.

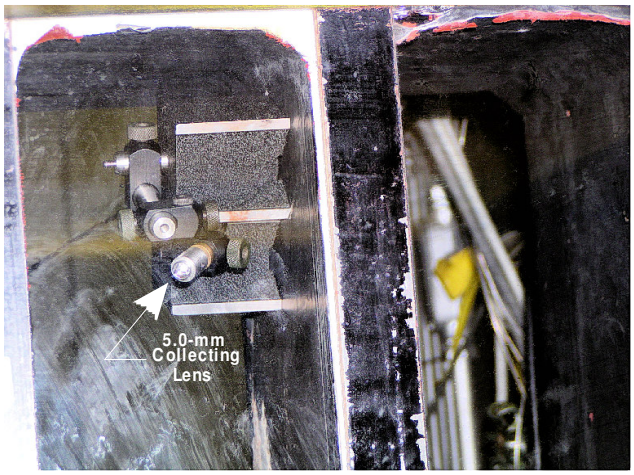

Figure 7.- Component B collecting lens.

3. System Calibration

Along with the geometric settings of the optical components and their measurements, DGV requires the optical frequency-energy transmission profile of the Iodine vapor cell to be calibrated along with the overall optical transmission characteristics of each measurement component. The Iodine cell was manufactured with a cold finger placed in a water bath set to 40° C to establish the internal vapor pressure. The cell body was heated above 60° C to insure that the cold finger was the controller. After 24-hours, the cold finger was sealed next to the cell body leaving only Iodine vapor within the cell. Thus when the cell is heated to 40° C or higher all of the Iodine would be in vapor phase, and thus there is no change in the optical frequency-energy transmission profile with small changes in temperature. This *vapor-limited* cell was routinely operated at 60° C. In the past, the calibration of the profile was attempted in various ways: 1) mode-hopping an Argon ion laser, 2) rotating wheels to impose a Doppler shift, and 3) high-frequency Bragg cells. The most accurate method found was to use a single-frequency, frequency-doubled Yb:YAG laser that generates a continuous wave green beam that can be tuned to match any of several iodine vapor absorption lines. The laser was tuned to the same absorption line as used with an Argon ion laser and located at the background level adjacent to the line. The laser was then tuned in 20 MHz steps throughout the absorption line and data acquired to define the optical frequency transmission profile. The laser light was monitored by a high-resolution wavemeter to provide a cross-check of the optical frequencies. The resulting calibration is compared to a prediction code developed by Forkey *et al* (1997) in Figure 8.

To obtain accurate measurements, the optical transfer function of the DGV system must be established. This transfer function is used to align the signal and reference pixel amplitude ratios

with the unity full-scale calibration of the Iodine vapor cell. It also yields the characteristics of the transmission and receiving optical systems, as well as the scattering characteristics of the particles in the flow. The transfer function must be obtained *in situ* under normal test conditions because of the Mie scattering sensitivity to particle size and viewing direction. Additionally, repeatability in particle size distribution from run to run cannot be assumed. The transfer function is obtained by shifting the laser frequency such that the Doppler shifted scattered light frequency lies outside of the Iodine absorption line where the calibration is unity. The measured signal / reference ratio is then used to normalize the measured ratios when the laser is shifted back to the optical frequency required for measurements, thus matching the Iodine calibration. Typically this is not an issue because these *flat field* measurements are obtained in free stream conditions. However, in the boundary layer investigation the velocity range extends from zero to free stream velocity. Thus the frequency shift must be large enough to move the entire Doppler frequency range outside the absorption line. This is easily accomplished with the tuning capabilities of the frequency-doubled Yb:YAG laser. However, only days before the first tunnel entry, the Yb:YAG laser failed with a catastrophic plumbing problem which caused several key optical elements including the laser disk to become damaged. Because this problem could not be repaired, an Argon ion laser was pressed into service and the optical system was correspondingly reconfigured. The limited optical frequency scan capability of the Argon laser necessitated the development of data correction techniques to obtain the *flat field* ratios for each pixel throughout the boundary layer. Additionally the available laser power was reduced by a factor of five as compared with the Yb:YAG.

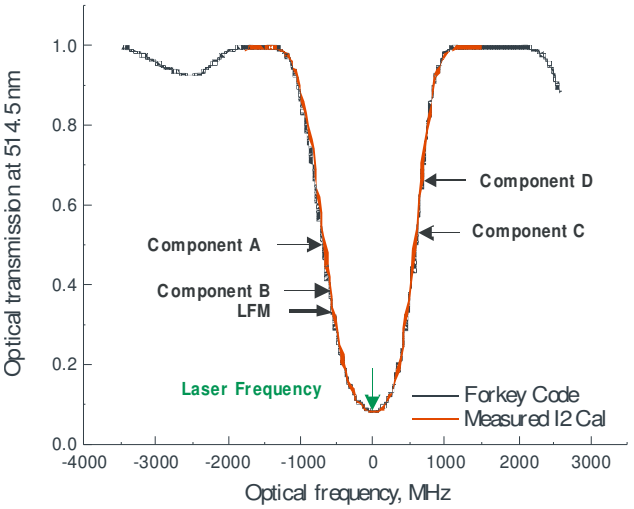

Figure 8.- Iodine vapor absorption and predicted Doppler shifts at Mach 3.51.

4. Implementation Issues

The first tunnel entry was devoted to investigating the boundary layer flow at Mach 1.51 and Mach 2.16. The four scattered light collecting optical systems were arranged in a symmetric pattern above the plane of the flat plate, Figure 4. The laser was tuned to the minimum point within the absorption line. The negative Doppler frequency shifts for components A and B would put the measured frequencies on the left side of the absorption line, Figure 8. The positive Doppler shifts for components C and D would put the measured frequencies on the right side. With the laser frequency at the bottom of the absorption line, its frequency could not be measured. Thus a laser frequency monitor (LFM) was constructed to obtain a 540 MHz frequency shift from a 270 MHz Bragg cell by passing the beam through the cell twice. The result was to move the sampled laser frequency 540 MHz to the left side of the absorption line center where it could be measured.

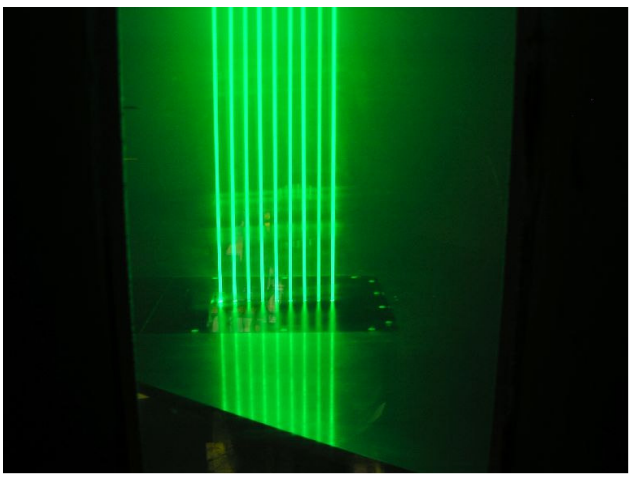

Figure 9.- Laser beam fence during testing at Mach 3.51.

Once the tunnel was brought to the desired operating conditions and before seeding, background images were acquired that provided the levels of laser flare from the model and tunnel structures along with normal background light. These images were subtracted from the data images to eliminate the effect of flare on the velocity measurements. However, once the seeding was injected into the flow, Figure 9, three more potential sources of measurement error became apparent. First, that the areas between the laser beams are not dark. This was caused by secondary scatter, i.e., light scattered from particles within the laser beams re-scattering from adjacent particles and producing unknown resultant Doppler shifts (Röhle and Schodl (1994)). This error was corrected by determining the scattered light intensities between the beams and extrapolating the trends as estimates of the intensity levels within the beams. These estimates were then subtracted from their respective signal and reference images in the same manner as the background light. Another consequence of secondary scattering originated from the illuminated particles returning light to the injection ports which caused an increase in the flare. This flare exceeded that determined from the background images even to the point of full pixel saturation, an effect not observed during laboratory mock-up tests. Finally, the black paint did not reduce the surface reflections of the light beams to the levels expected. The surface reflections also affect the intensity levels obtained near the injection ports which resulted in the inability to establish the exact location of the model surface within the data images. Instead, the surface location was determined from the background images because of the lower reflected light levels.

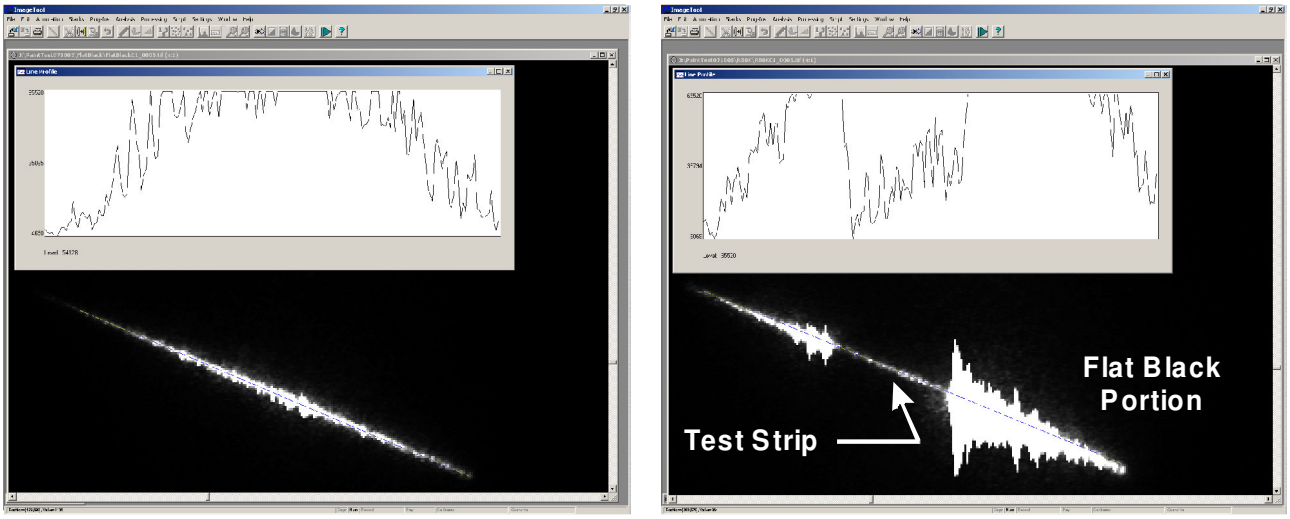

Figure 10.- Laser light scattering characteristics of two paints.

During the few weeks between the low-speed and high-speed tunnel runs, problems related to secondary reflections from the injection orifices and model surface were addressed. The flat black paint was replaced with Chroma-Base Black gloss paint impregnated with Rhodamine 590. A laboratory comparison of the scattering properties of the two paints is shown in Figure 10, with the impregnated paint reducing the flare by two orders of magnitude. The change in paint had a marked effect on the amount of flare originating from the injection orifices, though it was not reduced to negligible levels, Figure 11.

5. Post Test Challenges

Limitations in the time allocated for this portion of the test, (three days in the low-speed section and one day in the high-speed section) prohibited the implementation of any corrective procedures

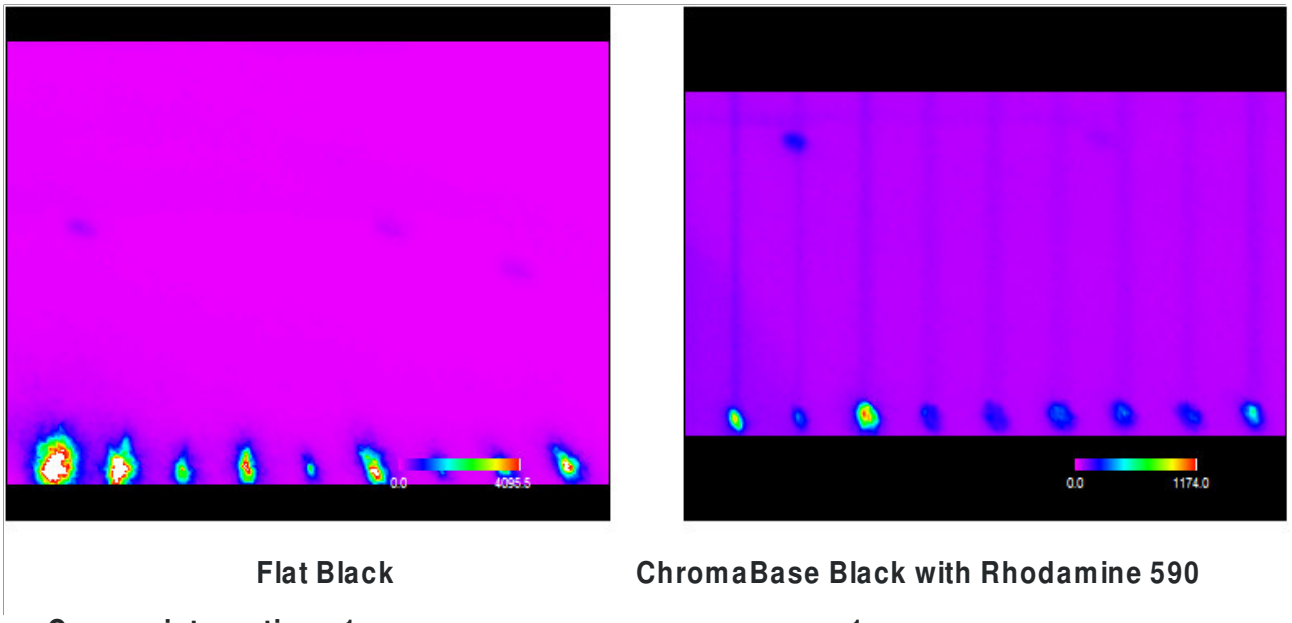

Figure 11.- Background images obtained from the two paints, Component B.

during testing. As such, corrective procedures were developed for use during data processing to minimize the effects from the Argon ion laser, secondary scatter, and flare from the injection orifices along with finding and hopefully correcting any other artifacts found during processing. A few of these problems were solved rather easily such as the particle-to-particle secondary scatter mentioned above and the elimination of the effects from the edges of the Gaussian beams. The high-slope intensity variations at the beam edges cause significant errors when minor misalignments exist between the signal and reference images. These errors were negated by integrating the collected scattered light along each pixel row within the limits of each beam. The integrated signal energy would then be normalized by the corresponding integrated reference energy to yield a single ratio for that pixel row, placed at the center location of that beam. Other problems proved to be more challenging.

The use of the Argon ion laser prohibited shifting the laser frequency to a point outside the Iodine absorption line. This forced the *flat field* measurements to be obtained with the Doppler shifted scattered light originating from within much of the boundary layer putting the resultant optical frequencies within the absorption line. Fortunately, the accuracy of the absorption line calibration, measurements by the monitoring high-resolution wavemeter, and the over-specified optical system provided sufficient information to build the *flat field* image. The only assumption made was that the flow was primarily directed downstream throughout the boundary layer.

A close inspection of the signal levels along the beams obtained in the high speed test revealed a nearly linear loss of signal strength beginning at the top of the boundary layer as the model surface was approached, Figure 12A. If there is a deviation from this trend observed by another component, then that deviation would most likely be caused by scattered light from the injection orifice, Figure 12B. Since component A (Figures 4 and 12A) views the beam from only a few degrees above the surface plane, it would not view inside the orifice whereas component B (Figures 4 and 12B) is viewing the surface from near the top of the test section. Thus, based on the trends found in component A, the near linear portions of the signal profiles could be extrapolated until the surface was reached, thereby eliminating the artifacts (red traces in Figure 12). This approach was also applied to the low speed data where the scattered light from the orifices was more intense, even to the point of saturating the pixels and causing pixel bleed.

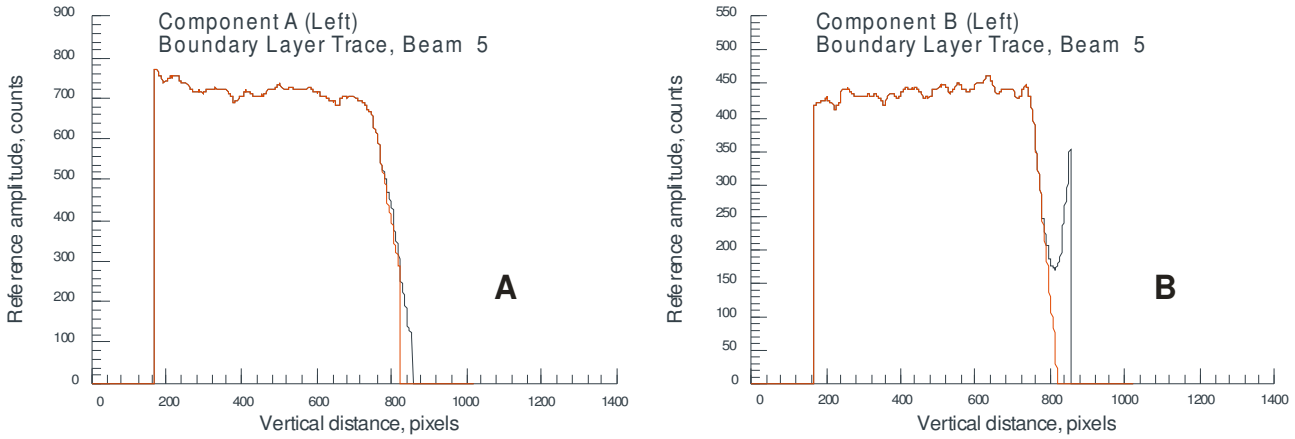

Figure 12.- Reference signal level profiles at Mach 3.51.

6. Discussion of Results

Although there is normally a decrease in particle number density within a boundary layer, the steep slope of the near linear behavior found in the signal strength profiles appeared to be beyond what would be expected. Comparing the Mach 3.51 results with the Mach 2.16 results finds that the termination of the signal was further from the surface, 3.2 mm versus 0.5 mm. The Mach 1.51 results found the distance increased to 25 mm above the surface with significant signal loss when the heat pulse was present. This behavior suggests that the number of seed particles decreased when the flow temperature rose, apparently through evaporation.

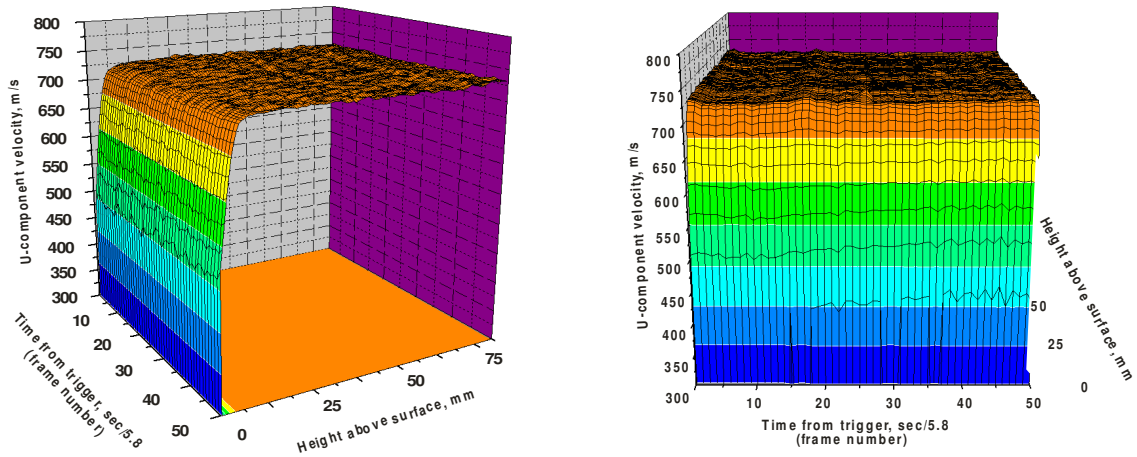

Figure 13.- U-component velocity – Mach 3.51, steady state.

Example time history results from a single laser beam are shown for steady state and heat pulse injected flows at Mach 3.51 in Figures 13 and 14 respectively. As expected the boundary layer flow appears to be stationary with time for the steady state condition, but oscillates with the passage of the heat pulse as it cycled around the tunnel circuit. An interesting point to note is that the velocity perturbation caused by the heat pulse changes phase by 180 degrees within the boundary layer. These same characteristics are found in the Mach 2.16 results, Figures 15 and 16. The results at Mach 1.5 show a noisy flow at steady state (Figure 17); however, unusable signals were found when the heat pulse was injected and thus no data was obtained. A transition from Mach 1.5 to 2.16, Figure 18, shows not only the increase in velocity with time, but measurements were obtained closer to the surface as the tunnel velocity increased.

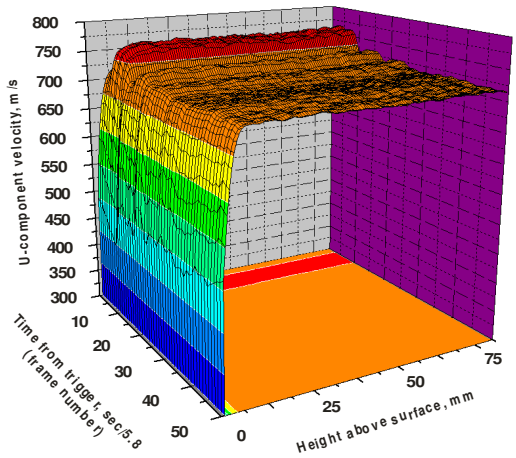

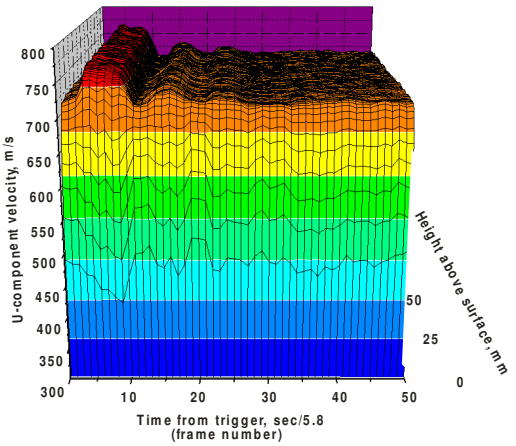

Figure 14.- U-component velocity – Mach 3.51, injected heat pulse.

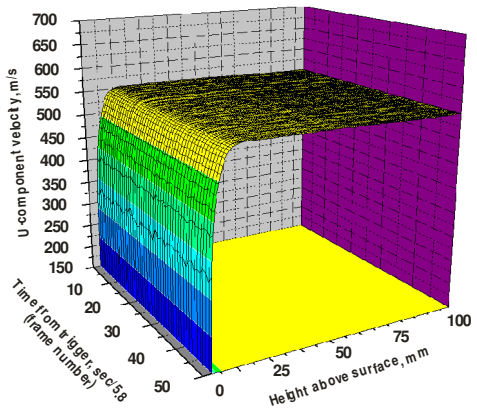

Figure 15.- U-component velocity – Mach 2.16, steady state.

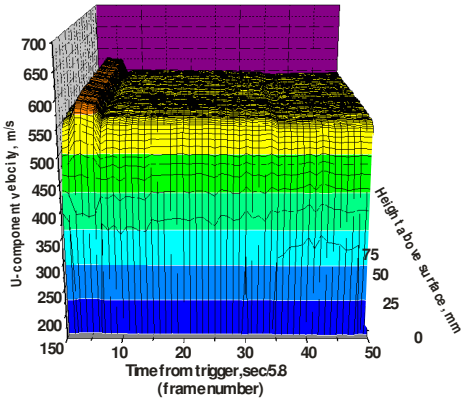

Figure 16.- U-component velocity – Mach 2.16, injected heat pulse.

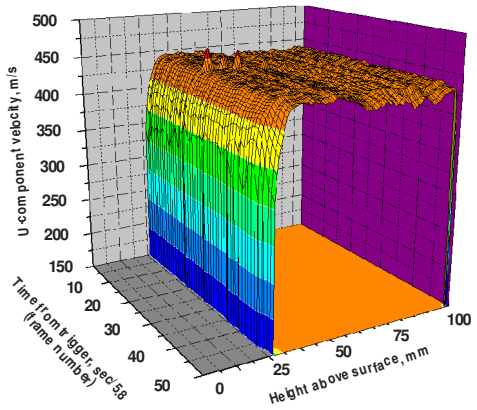

Figure 17.- U-component velocity – Mach 1.51, steady state.

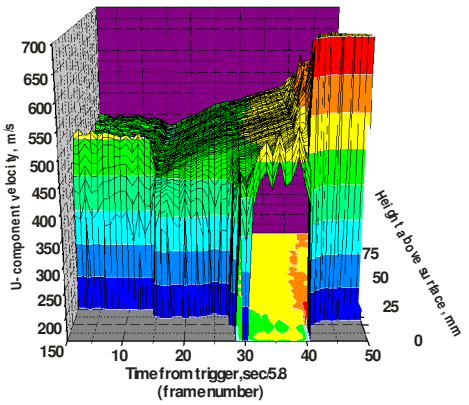

Figure 18.- U-component velocity – Mach 1.5 → Mach 2.16.

7. Concluding Remarks

A laser velocimetry system based on DGV technology was developed that is capable of providing three-component velocity measurements within a boundary layer in a supersonic flow. The system used multiple optical fibers to transmit laser light underneath the surface of a flat plate model. Output beams were transmitted through surface pressure port-sized (1.6 mm) orifices in the model surface to produce a series of laser beams perpendicular to the model aligned with the tunnel center-line. Scattered light generated by the passage of 0.1-micron condensation ice crystals was collected by four 5-mm diameter lenses attached to fiber-optic bundles which transmitted the collected light to a single, standard two camera DGV receiver. This system was used to investigate the boundary layer above a flat plate in a supersonic flow. The objective was to determine the effects of an injected heat pulse on the boundary layer. The results indicate that there is an increase in velocity in the free stream when the heat pulse was present, but a corresponding decrease in velocity within the boundary layer. This proof-of-concept investigation yielded velocity measurements of the boundary layer to within 0.5-mm of the surface at Mach 3.51 with no more impact on the flow than would be caused by standard pressure taps.

8. References

Brummund, U.; and Scheel, F.: *Characterization of a supersonic flowfield using different laser based techniques*. 10th International Symposium on Applications of Laser Techniques for Fluid Mechanics, paper 12.3, July 10-13, 2000.

Forkey, J.N.; Lempert, W.R.; and Miles, R.B.: *Corrected and calibrated I_2 absorption model at frequency-doubled Nd:YAG laser wavelengths*. Applied Optics, Vol. 36, Issue 27, pp. 6729-6738, 2007.

Herring, G.C.: *Mach-Number Measurement with Laser and Pressure Probes in Humid Supersonic Flow*. AIAA Journal, vol. 46, no. 8, August 2008, pp. 2107-2109.

Lowe, K.T.; and Simpson, R.L.: *An advanced laser-Doppler velocimeter for full-vector particle position and velocity measurements*. Meas. Sci. Technol. 20 (2009).

Meyers, J.F.: *Doppler global velocimetry measurements of supersonic flow fields*. VKI-Lecture Series 2005-1, Advanced Measurement Techniques for Supersonic Flows, ISBN 2-930389-57-5, February 28 – March 3, 2005.

Meyers, J.F.; Lee, J.W.; and Cavone, A.A.: *Doppler Global Velocimetry*. **Springer Handbook of Experimental Fluid Mechanics**, Tropea, C.; Yarin, A.L.; and Foss, J.F. (Eds.), Springer Verlag, Berlin Heidelberg, Chapter 5.3.4., pp. 342-353, 2007.

Meyers, J.F.; Lee, J.W.; Fletcher, M.T.; Cavone, A.A.; and Viramontes, J.A.G.: *Supersonic flow field investigations using a fiber-optic based Doppler global velocimeter*. 13th Int. Symp on Applications of Laser Techniques to Fluid Mechanics, Lisbon, Portugal, paper 1019, June 26-29, 2006.

Mangalam, S. M.; Dagenhard, J. R.; Hepner, T. E.; and Meyers, J. F.: *The Görtler instability on an airfoil*. AIAA 23rd Aerospace Sciences Meeting, Reno, NV, paper AIAA-85-0491, January 14-17, 1985.

Mangalam, S. M.; Meyers, J. F.; Dagenhard, J. R.; and Harvey, W. D.: *A study of laminar separation bubble in the concave region of an airfoil using laser velocimetry*. Proceedings of the Symposium on

Laser Anemometry, 1985 Winter Annual Meeting, ASME Fluids Engineering Division, Miami, FL, November 17-21, 1985, pp. 265-272.

Raffel, M.; Willert, C.E.; Wereley, S.T.; and Kompenhans, J.: **Particle Image Velocimetry - A Practical Guide**. Springer-Verlag, Berlin Heidelberg, 1998, 2007.

Röhle, I. and Schodl, R.: *Evaluation of the Accuracy of the Doppler Global Technique*. Proc. Optical Methods and Data Processing in Heat and Fluid Flow London, pp. 155-161, 1994.

Seiler, F.; Havermann, M.; George, A.; Leopold, F.; and Srulijes, J.: *Planar Velocity Visualization in High-Speed Wedge Flow using Doppler Picture Velocimetry (DPV) compared with Particle Image Velocimetry (PIV)*. Journal of Visualization, Vol. 6, No. 3/2003, pp. 253-262, 2003.